mSAIL: Milligram-Scale Multi-Modal Sensor Platform for Monarch Butterfly Migration Tracking

Inhee Lee^{1*}, Roger Hsiao^{2*}, Gordy Carichner², Chin-Wei Hsu², Mingyu Yang², Sara Shoouri², Katherine Ernst², Tess Carichner², Yuyang Li¹, Jaechan Lim², Cole R. Julick³, Eunseong Moon², Yi Sun², Jamie Phillips⁴, Kristi L. Montooth³, Delbert A. Green II²,

Hun-Seok Kim², and David Blaauw²

inhee.lee@pitt.edu,{rogerhh,gordyc,chinweih,mingyuy,sshoouri,katiesoo,carichnt}@umich.edu, yul230@pitt.edu,jaechan@umich.edu,cjulick@huskers.unl.edu,{esmoon,sunyeecs}@umich.edu, jphilli@udel.edu,kmontooth2@unl.edu,{dgreenii,hunseok,blaauw}@umich.edu

¹University of Pittsburgh, Pittsburgh, PA, USA, ²University of Michigan, Ann Arbor, MI, USA,

³University of Nebraska - Lincoln, Lincoln, NE, USA, ⁴University of Delaware, Newark, DE, USA

*Both authors contributed equally to this research.

ABSTRACT

Each fall, millions of monarch butterflies across the northern US and Canada migrate up to 4,000 km to overwinter in the exact same cluster of mountain peaks in central Mexico. To track monarchs precisely and study their navigation, a monarch tracker must obtain daily localization of the butterfly as it progresses on its 3-month journey. And, the tracker must perform this task while having a weight in the tens of milligram (mg) and measuring a few millimeters (mm) in size to avoid interfering with monarch's flight. This paper proposes mSAIL, $8 \times 8 \times 2.6$ mm and 62 mg embedded system for monarch migration tracking, constructed using 8 prior customdesigned ICs providing solar energy harvesting, an ultra-low power processor, light/temperature sensors, power management, and a wireless transceiver, all integrated and 3D stacked on a micro PCB with an 8 × 8 mm printed antenna. The proposed system is designed to record and compress light and temperature data during the migration path while harvesting solar energy for energy autonomy, and wirelessly transmit the data at the overwintering site in Mexico, from which the daily location of the butterfly can be estimated using a deep learning-based localization algorithm. A 2-day trial experiment of mSAIL attached on a live butterfly in an outdoor botanical garden demonstrates the feasibility of individual butterfly localization and tracking.

CCS CONCEPTS

• Computer systems organization \rightarrow Embedded hardware; Embedded software; • Information systems \rightarrow Sensor networks; Global positioning systems.

Permission to make digital or hard copies of all or part of this work for personal or classroom use is granted without fee provided that copies are not made or distributed for profit or commercial advantage and that copies bear this notice and the full citation on the first page. Copyrights for components of this work owned by others than ACM must be honored. Abstracting with credit is permitted. To copy otherwise, or republish, to post on servers or to redistribute to lists, requires prior specific permission and/or a fee. Request permissions from permissions@acm.org.

ACM MobiCom '21, January 31-February 4, 2022, New Orleans, LA, USA © 2022 Association for Computing Machinery.
ACM ISBN 978-1-4503-8342-4/22/01...\$15.00

https://doi.org/10.1145/3447993.3483263

KEYWORDS

miniaturized light weight sensing platform, energy harvesting wireless sensor, sensor fusion localization, animal migration tracking

ACM Reference Format:

Inhee Lee^{1*}, Roger Hsiao^{2*}, Gordy Carichner², Chin-Wei Hsu², Mingyu Yang², Sara Shoouri², Katherine Ernst², Tess Carichner², Yuyang Li¹, Jaechan Lim², Cole R. Julick³, Eunseong Moon², Yi Sun², Jamie Phillips⁴, Kristi L. Montooth³, Delbert A. Green II², Hun-Seok Kim², and David Blaauw². 2022. mSAIL: Milligram-Scale Multi-Modal Sensor Platform for Monarch Butterfly Migration Tracking. In *The 27th Annual International Conference on Mobile Computing and Networking (ACM MobiCom '21), January 31-February 4, 2022, New Orleans, LA, USA.* ACM, New York, NY, USA, 14 pages. https://doi.org/10.1145/3447993.3483263

1 INTRODUCTION

Animal migrators are critical ecosystem indicators because their long-distance travels, often on continental scales, integrate information over broad and diverse geographical locales and seasonal time scales. Tracking technologies have allowed us unprecedented access to these paths, offering insights not only into how migration works, but also into how environments are changing and how species interactions are impacted by changing movements and distributions [43]. However, currently only the larger animal migrators can be tracked for significant portions of their migratory flight (e.g. [52]). Long-term tracking devices require large amounts of energy and power for information processing and storage and large transceivers and antennas for data transmission, all of which increase the size and weight of the system. This makes them unsuitable for insect migrators, which make up a large percentage of the total abundance of migrators (e.g., 2.1 billion birds between Europe and Africa versus 3.4 trillion insects over the southern United Kingdom alone) [16]. Insect migration detection has been limited to en masse detection by vertical-looking entomological radar (e.g. [8]) or tracking for short periods of time or over short distances (e.g. [44, 45, 54]). Thus, the ability to track small individual migrators over their entire migratory path will offer a tremendous advance in our understanding of migration biology, the impacts of changing climate on small migrators, and effects of migrants on local and global ecosystems.

One of the most enthralling animal tracking stories has been that of the iconic eastern North American Monarch butterfly (*Danaus plexippus*). Each fall, millions of monarchs across the US and Canada migrate up to 4,000 km to overwinter in the same cluster of mountain tops in central Mexico. In spring, these migrants mate and remigrate northwards to repopulate their northern breeding territory over 2–4 partially overlapping generations. Because each migrant monarch completes only part of this round trip, and does not return to the overwintering site, this navigational task cannot be learned from the prior generation or involve commonly employed systems such as path integration, landmark-guidance, or (magnetic field) imprinting [31].

The number of monarchs completing the journey has steadily declined in the past decades, coincident with the decreased availability of their milkweed host plant [4]. The US, Mexico, and Canada have invested tremendous resources into monarch conservation efforts, including enacting specific policy initiatives, public outreach programs, and habitat protection and restoration projects. The US invested over \$11 million between 2015–2017 alone [37]. Developing a tracking technology for monarch can be key in these efforts, for instance through detailed understanding of habitat use during migratory flight and dependence on weather conditions. Furthermore, it can significantly benefit animal research, and agricultural and environmental science.

A monarch tracker must assure daily localization of the butterfly as it progresses on its journey while not interfering with its flight. As such, any deployed sensor must perform this task while having a weight in the tens of milligram (mg) and measuring a few millimeters (mm) in size. The conventional method for determining location is to use GPS. However, the received signal from the satellites is very weak (-155 dBm) and hence requires a power-hungry, very low noise amplifier (e.g. 25 mW by [34]). To power such a system requires, at minimum, a coin cell sized battery which by itself already weighs ~200 mg. Furthermore, the GPS carrier frequency of 1.58 GHz requires a relatively large, centimeter (cm) scale antenna. As a result, the smallest commercial GPS system (PinPoint by Lotek Wireless [32]) has a total weight of 1.1 g and size of 5 cm [15]. An alternate to GPS is the Motus system [49] which uses a radio beacon with tens of km transmit distance attached to each specimen combined with geographically distributed receive towers. However, while receive towers are relatively dense in Ontario and along the eastern seaboard, there are very few along the primary monarch migration region in the Midwest. Also, they require a long antenna (multiple cm) and have a weight >230 mg, which was found to significantly impede monarch flight [25]. Finally, daylight trackers were proposed to compute location based on sunrise/set times (e.g. Intigeo by Migrate Technology [21]). However, their data readout requires physical access to the sensor which is impractical in the case of monarch migration. Furthermore, their size/weight (320 mg and $12 \times 5 \times 4$ mm) remain well beyond that required for the monarch and, with only daylight-based sensing, location accuracy is limited, especially during the equinox.

Monarchs do not migrate in flocks as many bird migrators do. Rather, they primarily migrate as individuals, although sometimes monarchs are seen in large groups as they cross geographical barriers (e.g. crossing large bodies of water). One of the longer-term objectives of this work is to achieve understanding of how variable

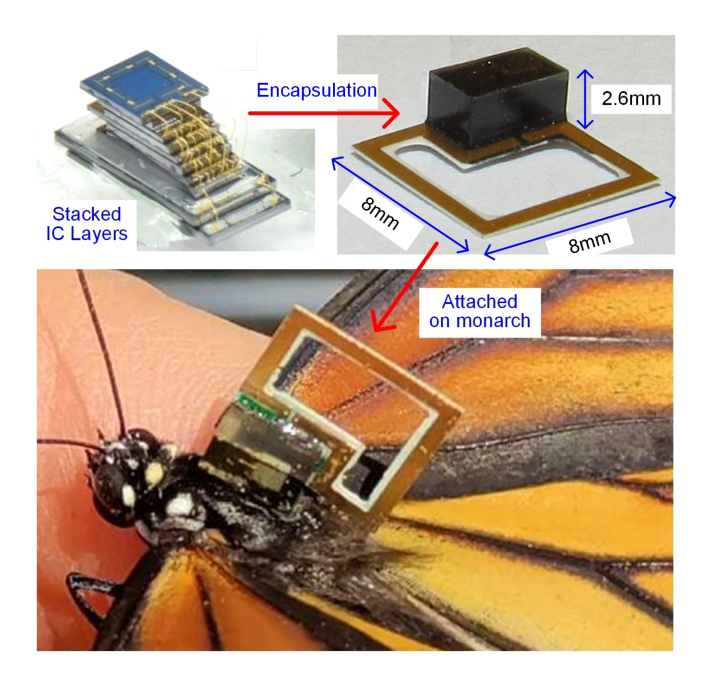


Figure 1: Proposed embedded system, mSAIL.

the individual paths are, as this will inform the type of navigational system that they employ on their trip (e.g. vector-based vs. true map-based). Tracking the mass (e.g. [8, 44, 45, 54]) has several limitations in determining how monarchs utilize different habitats and resources along their migratory flight. Also, for the same reason, a distributed approach with cameras or other sensors is not effective although there are 35,122 Monarch Waystations, as of July 13, 2021, across US, Canada, Mexico, and the Caribbean. Recently, a distributed approach with a radio transmitter on monarchs [25] utilized the Motus Wildlife Tracking System, an automated radiotelemetry network of over 100 towers. While an important advance, this small number of towers severely limits the coverage of signal detection.

We propose a new wireless sensing platform, mSAIL¹ (Fig. 1), specifically designed for the monarch migration study based on previously developed custom-designed ICs. mSAIL is an energy-harvesting, 62 mg device with a 8 × 8 × 2.6 mm form-factor (including antenna), that 1) simultaneously measures light intensity and temperature using non-uniform temporal sampling; 2) compresses the recorded data in 16 kB memory; and 3) wirelessly communicates data up to 150 m distance using a crystal-less radio at the overwintering site in a realistic non-line of sight (NLOS) scenario to custom designed gateways. An integrated, chip-size battery, continuously recharged using a custom-designed light-harvesting IC with eight photovoltaic (PV) cells, provides energy autonomy.

mSAIL addresses the following major technical challenges:

• Millimeter & milligram form factor: mSAIL must be small and light in order to not interfere with monarch flight and accurately record migration paths. A monarch weighs approximately

¹The platform as a whole as well as individual chips are available at cost to other researchers. Contact information, trained neural network models, and volunteer-collected data are available at: https://github.com/sarashoouri/Monarch_Butterfly_Tracking.

500 mg and has a thorax that measures approximately 8 mm long by 3 mm wide. Therefore, in order for the wings to properly close, a tagging unit must be <3 mm wide and to avoid restricting movement, it must be no more than 8 mm long. For vertebrate animals, weight for animal bio-loggers is typically <5% body weight [5]. However, insects can carry significantly more weight [25] and our preliminary respiratory study (Section 7.3.1) indicates even <15% is still acceptable (75 mg), although weight should always be minimized to the greatest extent possible. mSAIL meets these stringent specifications through multiple techniques: instead of one large chip, we stack small dies of previously designed ICs to obtain a compact design; we thin each die to 100 µm thickness to reduce stack height; we use a custom designed chip-scale rechargeable battery that integrates in the same chip stack; we use a ULP radio removing the need for an RF-reference (typically >10 MHz) crystal; finally, our transmitter/antenna co-design enables a 8 × 8 mm antenna while achieving >150 m distance.

- Energy autonomy: The highly constrained form factor limits available battery size and thus its capacity to only 18 μ Ahr. Within this very limited energy budget, the tracking device must periodically record sensor data for 3 months and radio out data at the end. mSAIL minimizes energy by employing three different operation modes: sleep (218 nW), active sensing (86 μ W) and wireless communication (130 μ W), each with mode-specific power management. Sleep uses ULP data retention memory, light sensing, always-on 32 kHz real-time crystal oscillator. By maximizing sleep time (99.3%) average current draw is reduced to 201 nA at a battery voltage of 3.9 V. The custom GaAs PV IC is able to maintain battery charge at 5 klux and the battery capacity is sufficient to radio out all the data at the overwintering site.
- Limited data storage: mSAIL uses custom ultra-low-leakage (ULL) SRAM for static power reduction. However, the limited silicon area allows only 16 kB memory space for data storage. To minimize memory footprint of the 3-month migration, we compress light, temperature and time-stamp data using a dynamic sampling interval scheme which has finer data resolution around the sunrise/set that most accurately predicts monarch location. A combination of the data compression and dynamic sampling interval reduces the required memory space from 772 kB to 7.2 kB, making 3-month tracking feasible.
- Wireless communication: Since monarchs overwinter in dense clusters, often high up in trees, long distance (>100 m) wireless communication is essential. However, mSAIL imposes extreme constraints on antenna size (8 × 8 mm) resulting in low antenna efficiency of -8 dBi. In addition, the mm-scale battery can sustain a maximum current draw of only 60 μ A due to its high internal resistance. We address this challenge by using a custom sparse pulse position modulation transceiver IC which accumulates charge on a capacitor between pulses, enabling 3.3 dBm transmit power. However, the transceiver IC exhibits high carrier frequency uncertainty and offset because it operates without a RF-reference crystal (typically >MHz), nor a PLL, to reduce the system size, weight, and power. This makes narrowband wireless communications more challenging. We address this using a new 2D-FFT based carrierand sampling-frequency offset joint estimation algorithm on a USRP X310 [14] compatible, custom gateway for real-time RF communication.

2 MONARCH MIGRATION TRACKING APPLICATION SCENARIO

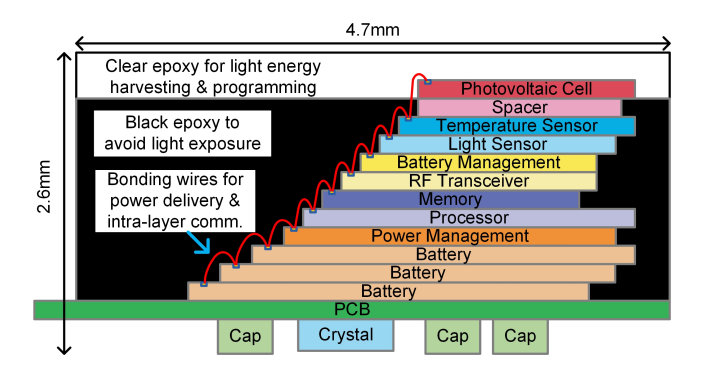
mSAIL records light intensity and temperature with accurate, 32 kHz crystal-based timestamps along the monarch migration path. Standard light-based locationing determines the sunrise and sunset time using a light intensity threshold and then determines the geolocation using a Sun-Earth system model [57] and Lambertian Law [56]. The day length and center time depend on the geolocation and date and has been used in long-term larger animal tracking studies [38, 46]. However, it has the fundamental limitation of large latitude ambiguity around the equinox (September 22 and March 20) when the day length is the same regardless of latitude. A second challenge is the significant light intensity variation due to weather and terrain that an ideal sunlight intensity model is unable to capture.

mSAIL adopts a novel data-driven algorithm for monarch migration tracking that leverages the principle of correlating multiple sensors. It achieves superior accuracy by applying deep neural network (DNN) models and multimodal fusion to effectively combine multiple sensor readings, including light intensity and temperature. The objective of the DNN approach is to identify cross-correlation between the multimodal readings and the sunlight intensity pattern as well as temperature information on a particular date. Different from [27, 28, 38] which utilize handcrafted models for light intensity and temperature, the DNN approach learns an implicit, yet more complicated model from real sensor measurements, which makes it more robust to local variations.

Although the details of the trajectory are not known, the final destination of the monarch migration is known. Overwintering monarchs will distribute over a limited number of sites within central Mexico with 21-78% of the total population reliably congregating at a single site (El Rosario sanctuary, at the Monarch Butterfly Biosphere Reserve) each year [53]. mSAIL nodes will be programmed with a predefined rendezvous time to start wireless data offloading to multiple gateways deployed at that overwintering site. This scenario allows retrieval from both fallen (dead) and live monarchs as long as they are within the communication range. Since an estimated ~90% of monarchs survive at the overwintering site [7, 50], the data recovery rate is expected to be significantly improved compared with current paper tagging methods [6, 35] that can only access dead butterflies. After a gateway retrieves the data log from an mSAIL, the entire butterfly trajectory can be constructed using the DNN localization algorithm proposed in [59]. The DNN is trained and evaluated by the data collected through a data measurement campaign with 306 volunteers from 2018-2020 across the US, Canada, and Mexico. They recorded light intensity and temperature using commercial cm-scale sensors [40] as an emulation of mSAIL during the monarch migration season. The localization algorithm [59] shows a geocoordinate accuracy of <0.6° and <1.7° in longitude and latitude respectively (1° is ~85.2 km in longitude and ~111.2 km in latitude in the midwestern US), which is sufficient for monarch studies.

3 SMALL FORM FACTOR INTEGRATION

This section discusses how mSAIL achieves a mm- and mg-scale form factor using 3D stacked custom ICs, batteries, and PCB antenna. mSAIL measures $8\times8\times2.6$ mm and 62 mg to not interfere



Components	Size (mm)	Weight (mg)	Sleep Power (nW)	Feature
Photovoltaic-cell IC	1.35×1.53×0.15	0.7	N/A	8 large and 3 small cells, GaAs
Spacer	1.05×1.33×0.10	0.3	N/A	Light blocking
Temp. Sensor IC	1.05×1.63×0.10	0.4	0.03	ULP temp-to-digital conversion
Light Sensor IC	1.05×1.63×0.10	0.4	35.0	ULP light-to-digital conversion
Battery Management IC	1.05×1.93×0.10	0.5	0.04	Battery protection, nF decaps
RF Transceiver IC	1.35×2.08×0.10	0.7	1.85	ULP RF transceiver
Memory IC	1.35×2.23×0.10	0.7	1.32	16kB ULL SRAM memory
Processor IC	1.35×3.10×0.10	1.0	3.48	ARM Cortex-M0, 16kB memory
Power Management IC	1.35×2.55×0.10	0.8	145	Power conversion from battery
3 Batteries	1.35×2.83×0.20	1.8	N/A	Lithium, Thin-film, 6µAhr each
PCB	8.00×8.00×0.10	19.5	N/A	Rogers 4350B
Crystal	1.27×1.05×0.50	2.0	N/A	Seiko SC12S-7PF20PPM
3 Caps	0.60×0.30×0.55	0.6	N/A	4.7µF & 1.3pF

Figure 2: mSAIL structure and layer information.

with monarch flight, while still providing necessary features as a complete system. It consists of three main parts: stacked IC layers, a PCB, and discrete components.

3.1 Stacked Custom IC Layers

mSAIL consists of a family of bare-die (without packaging) IC layers. Fig. 2 shows the layers: a PV cell IC, a ULP processor and memory IC, ULP temperature and light sensor ICs, a ULP RF transceiver IC, and a battery/power management IC, which were all custom-designed, fabricated and thinned. Three custom-designed, thin-film batteries [11] are also stacked as additional layers. To minimize the total system volume, the layers are stacked on top of each other and connected by bonding wires. The layers communicate using a custom low-power protocol called *mBus* [26, 41, 42].

3.1.1 Processor & Memory Layers. These layers are the heart of mSAIL and include a ULP ARM Cortex-M0 processor and a custom ULL 16 kB SRAM. For average power reduction, the overall system is heavily duty-cycled, turning off all unnecessary components in the 1 to 8 minute sleep intervals between light/temperature readings. Only essential blocks remain turned on: a power management unit, memory, a continuous integrating light sensor [30], and a 5.6 nW 32 kHz crystal oscillator [60]. During a short 1.2 s active mode, it reduces energy to 9.4 pJ/OP using near-threshold computing [1, 13, 61], by running the processor at 0.6 V. It limits the maximum current draw from the battery to <60 μ A to avoid a large voltage drop from the high internal resistance of the small battery (6.7 k Ω). The memory layer provides an additional 16 kB SRAM for data storage. Both memory in the processor and the memory layer use a custom designed bitcell with lowest-in-class standby power (3.35 fW/bit) [39].

3.1.2 Temperature & Light Sensor Layers. The temperature sensor layer converts temperature to a digital code by counting pulses from a temperature-sensitive oscillator referenced to a temperature insensitive clock signal [22, 58]. It achieves a temperature resolution of 0.1 $^{\circ}$ C from 0 to 105 $^{\circ}$ C. Since temperature changes slowly, it is only read during active mode and is then powered off to save energy.

Light levels, however, can vary significantly in short periods of time (e.g. due to shading). Therefore, the light sensor layer is always on and integrates charge from a small PV cell on the PV cell layer and converts the averaged value during long sleep periods to a digital code [30]. The light sensor consumes only 35–339 nW, depending on the light level, with the highest power occurring during full incident sunlight when abundant energy harvesting easily offsets this higher power consumption. It achieves an accuracy of ±3.8% and a range of <1 lux (twilight) to 300 klux (direct sunlight).

3.1.3 RF Transceiver Layer. To achieve long distance communication, a high transmit power (mW range) and a high efficiency antenna are necessary due to the basic physics of RF signal propagation. Typically, however, high power requires large batteries with low internal resistance and an efficient antenna requires large size. A custom ULP RF design [10] addresses the high transmit power challenge (which cannot be sustained by our small battery) by sending a sequence of short, high-power (3.3 dBm) RF pulses with sparse pulse-position modulation (PPM) using two discrete energy buffer capacitors which are trickle charged between pulses (Fig. 6). This sparse PPM enables >150 m NLOS communication with only 130 μ W of average power consumption but it sacrifices data rate (0.2 kbps) by spreading out the sparse pulses. However, mSAIL can still read out the complete data log (7 kB after compression) in ~27 minutes (including inter-packet idle time), which is acceptable in our application.

3.1.4 Battery Layer. mSAIL includes three rechargeable solid state thin-film lithium batteries [11]. Each battery is $1.35 \times 2.83 \times 0.2$ mm and has a charge capacity of 6 μ Ahr, providing a voltage from 3.6 to 4.2 V. Due to the small size, each battery has relatively large internal resistance of 20 k Ω at room temperature with three parallel batteries providing 6.7 k Ω . Thus the maximum current draw is limited to 60 μ A for the system's maximum tolerable voltage drop of 0.4 V from the minimum system operating voltage of 3.8 V.

3.1.5 Power Management Layer. The high battery voltage of $\sim\!4$ V cannot be directly applied to most of the circuits since the maximum allowable voltage of standard transistors in the 180 nm CMOS process used is 1.8 V. Also, to lower energy consumption, the power management layer converts the battery voltage down to 1.2 V and 0.6 V. The battery voltage varies depending on the state of charge stored in the battery and the battery's internal resistance leads to significant IR drop. A recursive switched-capacitor DC-DC converter [47] with all-on-chip capacitors and $\sim\!30$ mV output voltage resolution converts the varying battery voltage to a stable 1.2 V and then another 2:1 DC-DC converter generates the 0.6 V [23]. Software adjusts the conversion ratio for battery voltage droop, mode-specific current draw, and temperature dependent battery resistance. The power converters achieve conversion efficiency of 60–68% from 20 nW–500 μ W [23].

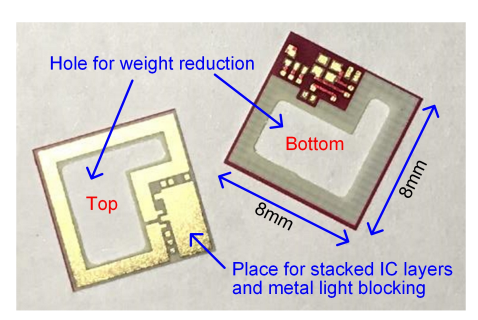


Figure 3: mSAIL PCB.

3.1.6 Photovoltaic Cell & Battery Management Layers. Although duty cycling and ultra-low standby power design yields an average power consumption of only 201 nA, the batteries of mSAIL can sustain the system for only 3.8 days without recharging. Hence, mSAIL extends the system lifetime and becomes energy autonomous by using a custom-fabricated energy harvesting IC with eight PV cells connected in series [29, 36]. Through the on-chip series connection, the layer generates a voltage higher than the battery voltage allowing it to directly charge the battery without need for traditional voltage up-conversion. This removes the need for a harvester layer and achieves a high electrical-efficiency of 70-90% from 400 lux to 30 klux. Constructed from GaAs, the PV cells have a high light to electricity efficiency of 26% [36]. The battery management layer prevents battery discharging at a low light condition with a diode between PV-cell output and battery while an over-charging protection circuit prevents the battery from being charged above 4.2 V. Since only an uncharged Li-battery can withstand the high temperatures during epoxy curing, the battery is kept uncharged through a PV-cell shorting wirebond which is later removed.

3.2 PCB and Antenna Design

mSAIL places the IC stack on a PCB (Fig. 3) with dimension of 8 \times 8 \times 0.1 mm, fabricated in a Rogers 4350B material. The weight of the PCB is reduced down to 19.5 mg with a large opening in the center of the a single loop trace antenna, which takes 38% of the PCB area. In addition to the IC layers, the PCB integrates two 4.7 μF and one 1.3 pF ceramic capacitors for the RF transceiver and a small 32 kHz crystal (1.3 \times 1.1 mm, 2 mg), used by the processor layer for system time keeping.

An antenna is traditionally designed in a size similar to the RF wavelength. A mm-scale antenna therefore requires a very high RF frequency in the range of tens of GHz, the generation of which can require enormous power consumption. Also, such an RF signal has a high path-loss and is easily blocked by obstructions. Instead, we choose a moderate frequency of 915 MHz (ISM) with excellent penetration characteristics and mild path-loss. However, a standard monopole or dipole antenna of 6 mm has a radiation efficiency of -35 dBi at 915 MHz [9] meaning <0.1% of power delivered to the antenna is radiated. To address this, mSAIL uses a magnetic loop antenna, which is >10× more efficient than an electric mono- or dipole-antenna when considering matching elements [10]. This antenna achieves a radiation efficiency of -8 dBi, which is low compared to conventional antenna designs, but outstanding for its size. By using longer pulses (50 μ s / 20 kHz bandwidth), mSAIL compensates for the lower antenna efficiency without incurring

an increase in the instantaneous current (or power) draw while still operating from two 4.7 μ F capacitors as energy buffers for sparse-PPM pulse transmission.

3.3 System Integration and Encapsulation

mSAIL integrates 12 layers, two 4.7 μ F capacitors for RF communication energy buffers, one 1.3 pF capacitor for RF frequency selection and a 32 kHz crystal on the PCB. They are electrically connected by PCB traces and bonding wires. The ULP ICs are stacked without conventional chip packaging (i.e., bare-die) after thinning, saving weight and size but rendering them extremely sensitive to light, and the bonding wires are very fragile. Thus, they must be properly encapsulated to provide physical protection and to block light. At the same time, the PV cell layer must be exposed to light to perform energy harvesting and light level measurement. To address these simultaneous integration constraints, the PV cell layer is placed on top of the other layers for access to light. The bottom layers are encapsulated with a hard, black epoxy to provide physical protection and block light from reaching the sensitive electronics. The top PV cell layer is covered by a clear epoxy to expose the PV cells to light. Below the PV cell layer, the spacer layer coated with aluminum blocks light coming through the PV cell layer. A silicone mold ensures the epoxy only surrounds the layers to not increase the total weight. Thus, its weight contribution is reduced to 27.9 mg, which is a 5.9× reduction compared if the epoxy had covered the entire PCB area. Finally, the entire mSAIL is coated by parylene, which is biocompatible, blocks moisture and electrically isolates conductive points on the PCB from the environment.

After encapsulation, mSAIL is programmed via optical communication using a portable LED shining on the exposed PV cells. The processor layer decodes on-off-key modulated (0.8 kbps) commands and programs the system accordingly.

4 ENERGY AUTONOMOUS OPERATION

mSAIL uses its PV cells to sustain the charge of its integrated batteries during the 3-month migration which have sufficient energy to power the wireless data transmission at the overwintering site. The system must minimize energy consumption, since the mm-scale batteries only store 18 μ Ahr of charge and the mm-scale PV cells only recharges the battery with 100 nW–20 μ W from 400 lux to 30k lux. The battery can only sustain 49 minutes if mSAIL continuously operates in active mode without careful energy management.

4.1 Dynamic Operation Modes

mSAIL optimizes energy consumption by employing three different operation modes: active, sleep, and radio. In active mode, it measures temperature, triggers light measurement, processes, stores and time stamps measured data, and re-configures the power management unit for optimal efficiency. The active mode consumes 22 μ A on average running for a duration of 1.2 seconds. For power reduction, the sleep mode turns off all circuits except for essential blocks: the 32 kHz crystal oscillator, the volatile SRAM memory, the light sensor, and power management. Also, it reduces the DC-DC converter clock frequency from 588 kHz to only 370 Hz to maintain a high power conversion efficiency of 66% at 56nA sleep mode current (29× efficiency reduction compared to if kept constant).

mSAIL is in sleep mode for from 98.0% around sunrise/set to 99.8% at the center of day and night. Due to the large period ratio of 150:1 between the sleep and active modes, the overall system energy consumption is substantially determined by the sleep mode.

After the monarch arrives at the overwintering site, mSAIL will wirelessly transmit all the stored data to a gateway at the predefined rendezvous time, consuming 130 $\mu \rm W$ on average. This consumes 211 mJ over 27 minutes, which must be supported by the integrated battery with energy capacity of 259 mJ. During the transmission, the processor monitors the batteries and if they cannot support the entire data transmission, mSAIL waits for the batteries to be charged to 3.9 V (detected by an integrated ADC) and then transmitts the remaining data at the next rendezvous time.

4.2 Adaptive Power Management

Power consumption of circuits changes across temperature. In particular, it changes significantly in sleep mode when the total power is dominated by the subthreshold leakage current, which exponentially increases with temperature. For reliable and energy-efficient operation, mSAIL periodically measures temperature and adaptively adjusts the frequency of switched-capacitor power converters. If a constant configuration is applied to the power converters for the entire temperature range (-10-60 °C), the system suffers from poor power conversion efficiency since the high frequency configuration for worst-case load current is used in other temperatures. mSAIL sets different converter frequencies to optimize DC-DC switching and conduction loss for seven temperature boundaries (-10, 0, 10, 20, 35, 45, 60 °C). In each range, the frequency is set based on characterized system load current plus margin. By using temperature specific settings, we increase worst-case DC-DC conversion efficiency by $2.4\times$.

4.3 Ambient Light Energy Harvesting

To recharge the batteries, mSAIL uses a PV cell layer. The battery voltage is \sim 4 V, and a single PV-cell outputs 0.5–0.85 V from 0.1 to 100 klux. To bridge the voltage difference, a typical system includes a DC-DC converter, such as an inductive boost converter or a switched-cap converter, to increase the low PV-cell voltage to the high-voltage battery. The inductive boost converter requires a high-Q bulky inductor with a size and weight not acceptable for mSAIL. A previous switched-cap converter IC [24] uses only on-chip capacitors. However, it suffers from lower conversion efficiency in the lower power range (e.g., 40–50% for 5 nA–5 μ A [24]) due to unavoidable internal circuit operation and switching loss.

In contrast, mSAIL generates high voltage by electrically connecting eight custom-designed PV cells in series and directly charges the batteries without any circuit operation or switching loss. The number of PV cells is set eight to place their effective maximum power point at a relatively low light level (500 lux–2 klux) so that energy harvesting is supported at these low light levels [29]. At stronger light levels, the harvesting efficiency decreases, but the absolute harvestable energy is much greater. While mSAIL could benefit from a large charging current at strong light, its energy harvesting efficiency is optimized at low light level to maximize the acceptable light range for energy harvesting. The battery voltage does not increase beyond 4.2 V because an overcharging protection

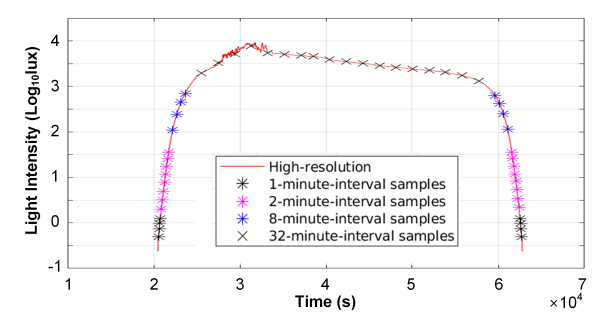


Figure 4: Sampled light with varying sampling rates.

circuit stops the energy harvesting, protecting the ICs as well as the battery [29]. At very low light levels (<100 lux), the energy harvester cannot provide enough voltage to charge the batteries and imposes a risk of discharging the battery instead. To prevent this problem, a diode is inserted between batteries and the output node of the PV cell layer [29]. This results in harvesting efficiency loss of 7% from the voltage drop across the diode during energy harvesting, which is easily compensated by the improved efficiency from not having an active up-converter.

5 DATA MANAGEMENT

Due to the silicon area constraint, mSAIL has a limited data storage capacity of 16 kB in custom ULL SRAM for the 3-month journey. For the DNN sensor fusion localization algorithm [59], measurement intervals of 1 and 32 minutes are desired for light and temperature, respectively. Temperature changes are gradual so the required measurement interval is much longer than the light recording interval since light levels can vary rapidly with weather or shading, and change exponentially around sunrise/set time. Since the temperature and light sensor outputs are encoded with 24 and 48 bits per measurement, respectively, storing raw data would require 772 kB of SRAM to store all the measurement data during the migration period, which is well beyond the 16 kB storage capacity. Thus, mSAIL reduces the data storage requirement by compressing the data using Huffman-coded, log-scale encoding with a nonuniform subsampling scheme guided by dynamic sunrise/sunset time tracking. The proposed data compression also reduces energy consumption for wireless data transmission at the overwintering site.

5.1 Dynamic Sampling Rate

The localization algorithm requires a light profile for the entire day [59]. However, temporal resolution around sunrise and sunset, where intensity level changes exponentially, is more critical. To reduce the power consumption and required memory space, mSAIL reduces the number of measurements by dynamically controlling the sampling rate. It measures the light every minute for 3 hours around sunrise and sunset and every 32 minutes otherwise, which reduces the storage size by roughly 4×. Data during the night is assumed to be 0 lux and is not stored. In addition, after the 3-hour window of 1-minute interval measurements is obtained, mSAIL further subsamples light measurements by applying gradually increasing sampling intervals. From the time when the light level crosses a threshold (e.g., 2 lux) and moving toward the center of day, it stores 4 samples at 1-minute intervals, 8 samples at 2-minute

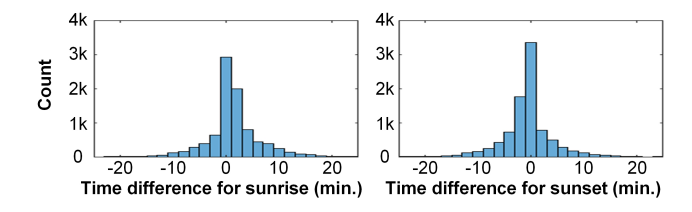


Figure 5: Histogram of relative time difference between consecutive sunrises and sunsets.

intervals, 4 samples at 8-minute intervals, and the rest of the 3-hour window is stored at 32-minute intervals (Fig. 4). This further reduces the storage requirement by 10×, without noticeable localization accuracy degradation (Section 7).

5.2 Sunrise and Sunset Tracking

To perform the proposed dynamic subsampling, mSAIL must track sunrise and sunset times which will change as the butterfly travels. Without dynamically tracking sunrise/set, 14 hours per day of 1-minute measurements would be necessary to cover all the possible sunrise/set times across different locations during the migration. Such a large window of high frequency measurement results in longer active times for processing data and higher energy consumption.

mSAIL predicts the sunrise and sunset times each day based on the previous day. We limit our discussion in this section to sunrise times for brevity, but the method applies similarly to sunset. The model can be described by the equation $T_n = T_{n-1} + \Delta T_{local} +$ ΔT_{alobal} where T_n is the time the light level crosses the threshold on day n. ΔT_{local} describes the local changes in sunrise time and light levels had the butterfly not traveled; this contains the changes from seasonal, weather, and shading variations. ΔT_{alohal} describes the changes in sunrise time due to global displacement of the butterfly. ΔT_{local} can be measured by the difference in the sunrise times between consecutive days at the same location in the reference volunteer dataset [59] shown in Fig. 5. We can pick 30 minutes as a reasonable upper bound of ΔT_{local} based on Fig. 5, whereas ΔT_{alobal} can be determined analytically. The maximum reported speed of a monarch butterfly is 265 miles per day [48]. This is a conservative estimate - a more typical value would be 50-100 miles per day. At 45 °N, 265 miles corresponds to about 5.5 degrees in latitude which shifts the sunrise and sunset times by ± 22 minutes in the worst case assuming that the butterfly travels only in the east-west direction. Therefore, $|\Delta T_{local}| \leq 30$, $|\Delta T_{global}| \leq 22$, and $T_n = T_{n-1} \pm 52$ holds. And if the 1-minute light measurement window is set to ± 52 minutes before and after the previous sunrise time, it is guaranteed to capture the next sunrise. The recorded samples require an addition 54 minutes after sunrise and, hence, the total window is set to 1 hour before and 2 hours after the previous sunrise time.

5.3 Data Compression

The dynamic sampling rate reduces the number of data points down to \sim 100 light and 48 temperature samples per day. Each raw light and temperature measurement is 48 and 24b long, respectively. To

compress both light and temperature data with the limited instruction code space and computational complexity, a compact lossy compression algorithm is applied to convert the integer data into an approximated log2 representation with fixed-point precision without using a large lookup table. Log2 representation is suitable for the light data as it changes exponentially around sunset/rise time. For approximated log calculation, mSAIL first determines the position of the leading 1 in the input value *X* to find the decimal part of the number. Then, it tests each fractional bit by constructing an approximation of X. Note that this algorithm only requires 5 precomputed values $(2^{\frac{1}{2}}, 2^{\frac{1}{4}}, ..., 2^{\frac{1}{32}})$ to achieve a resolution of $\frac{1}{32}$ in the log domain. This method compresses light measurements to 11b (6 decimal and 5 fractional bits) and temperature measurements to 7b (4 decimal and 3 fractional bits). The compressed data maintains its relative light resolution at 2.2% ($2^{1/32}$) and temperature resolution at 4.4% ($2^{1/16}$). After compression, all the data for 90 days occupies 15.7 kB of mSAIL memory.

Finally, data is further compressed by storing only the difference with the previous data. During sunrise and sunset, log-scale light intensity samples change by a relatively small amount (typically 1 or 2 bits). A Huffman coding [17] is applied to this difference to produce the minimum codeword length. The combined encoding scheme further reduces a light measurement to 5.1b and a temperature to 3.0b on average. A simulation on the volunteer-collected data shows that only 7.2 kB SRAM is required to store 3-month data including overhead, which is acceptable for the mSAIL.

5.4 Data Packets for RF Communication

During wireless data retrieval, each packet is separately transmitted and contains 96b including 16b of CRC and a 12b packet header. The remaining 68b store the data. To reduce overhead, four packets are grouped together (272b data) as an independent decodable unit. Each unit storing light measurements includes a 17b timestamp (with resolution down to 1 min) and an 11b initial measurement value (necessary for differential decoding). Units storing temperature measurements include a 13b timestamp (with resolution down to 30 min) and a 7b initial measurement. The remaining light and temperature measurements are stored as an encoded difference from the previous measurement as described in Section 5.3. The remaining timestamps are omitted as they are calculated at the gateway since the light and temperature intervals are deterministic, though non-uniform. Once mSAIL reaches the overwintering destination (inferred by the rendezvous time), mSAIL adds-on the packet number and CRC to each unit to create four 96b packets for transmission. The CRC enables multi-bit detection of erroneous packets in the receiving gateway. Although a missing packet cannot be recovered, the earlier packets can still be decoded using the timestamp and initial data stored in the first packet even if later packets are lost. Also, since mSAIL will periodically retransmit its data, lost packets can be recovered on subsequent data transmissions.

6 WIRELESS RF COMMUNICATION

Using a ULP RF transceiver without an RF-reference crystal (10 MHz range) and PLL [10] is necessary to enable mm-scale system integration and also ultra-low power consumption, but it unavoidably sacrifices frequency stability of the RF signal. To address this, the

system employs a gateway-assisted synchronization protocol that is initiated by mSAIL node transmission. In the proposed protocol, an mSAIL node asynchronously initiates a communication session by transmitting a packet first. Around the rendezvous time, the gateway continuously listens to the channel to estimate and track the carrier frequency and sampling frequency offsets (CFO and SFO) of the mSAIL node via a computationally efficient 2D-FFT based correlation. Upon detecting a valid packet from an mSAIL node, the gateway can send a customized packet that *pre-compensates* the CFO/SFO of the detected mSAIL node. This enables a PLL-less mSAIL node implementation which eliminates the need for powerdemanding synchronization/correlation processes at the mSAIL node. The gateway protocol and real-time baseband signal processing are implemented on the FPGA (ADRV9361-Z7035) of a custom gateway (USRP X310 compatible, Fig. 11). This asymmetric link between the gateway and mSAIL takes advantage of excellent receiver sensitivity and abundant FPGA resources for digital signal processing in the gateway, allowing the mSAIL transceiver to be simple, low power and mostly asleep.

A major issue of using a mm-scale battery for mSAIL is its high internal resistance, which prevents drawing large peak current (mA range) to transmit RF signals. Note that prior crystal-less transceiver designs such as [33] do not have the same issue as they operate with a conventional battery without an extreme size and weight constraint. We tackle this current limitation issue of the mmscale thin-film battery by powering the transceiver with a trickle charged energy buffer capacitor. Instead of pulling current directly from the battery, the transmitter pulls high instantaneous current from the capacitor to generate RF pulses as shown in Fig. 6. The battery is continuously recharged through the mm-scale PV cell and after each pulse transmission, the battery recharges the capacitor to its nominal voltage through an on-chip current limiter. Since the recharging time is much longer than the pulse duration, the transmitted pulses appear sparse in the time domain. The proposed system exploits this sparsity to realize an energy efficient sparse pulse position modulation (PPM) scheme. Unlike conventional PPM, the symbol duration is dominated by the recharging time. mSAIL uses a binary sparse-PPM with 2.25 mW active transmit power (at \approx 15% circuit efficiency), 50 μ s pulse duration, and 4.8 ms recharging time for 0.2 kbps data rate at an average power consumption of 156 μ W during the packet transmission.

The main challenge in the gateway design is to identify the CFO and SFO with the mSAIL node *in real-time*. On the mSAIL RF transceiver the baseband sampling clock is generated by a RC relaxation oscillator [10] and its carrier frequency is determined by the inductance value of the 2D magnetic dipole loop antenna and the matching on-/off-chip capacitors without a PLL. Thus, it is inevitable that an mSAIL node has significant SFO (up to 0.5%) and CFO (up to 2%) variation due in part to variations in process/voltage/temperature. Calculating accurate SFO/CFO and compensating these offsets in real-time is performed with the signal processing data path shown in Fig. 7 implemented on the gateway's FPGA.

The preamble from mSAIL always starts with an RF pulse train with *a constant pulse interval*. Thus, we propose a novel 2D-FFT based process that identifies the SFO and CFO at the same time.

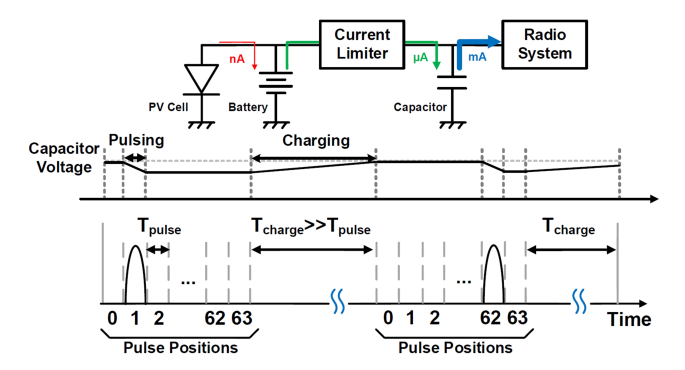


Figure 6: Modulation and recharging scheme.

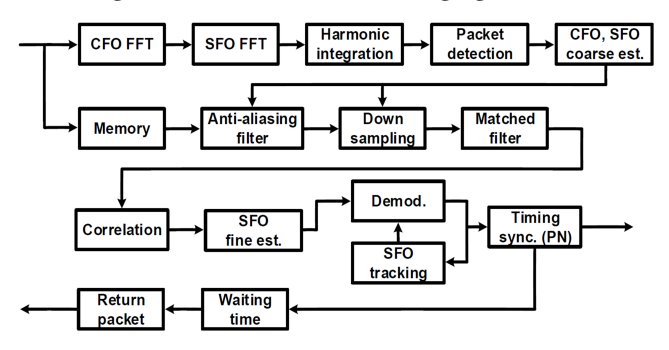


Figure 7: DSP datapath implemented on the gateway.

The incoming signal is first divided into multiple time domain signal frames, whose length is equivalent to half of the pulse width. A 1D-FFT is performed on each signal frame and signal power is computed for each frequency offset bin, which corresponds to a specific CFO hypothesis. A second FFT is then performed on the power of frequency domain samples (output of the first FFT) that belong to that same bin (one specific CFO). This process is repeated for all frequency bins. Each bin of the second FFT output now corresponds to a specific SFO fundamental frequency. To accurately estimate the actual pulse repetition frequency of the preamble, we add the power of all harmonic frequency bins corresponding to a specific fundamental frequency. Fig. 8 shows an example of the 2D-FFT harmonic integration output from the preamble processing, where the y-axis corresponds to the CFO bin and x-axis is the SFO fundamental frequency hypothesis. By finding the maximum power from the 2D-FFT result, the gateway identifies the SFO as well as the CFO at the same time. The CFO FFT resolution is matched to the signal bandwidth and inversely proportional to the preamble pulse width, which is 4 – 1000 μ s in our system. Fig. 8 is the result for $6.5~\mbox{MHz}$ CFO and 5 kHz SFO from the 915 MHz and 250 kHz ideal carrier and sampling frequencies (plotted with a coarser resolution to make the high power peak region visible). After the 2D-FFT process for preamble, the gateway keeps tracking SFO during payload to eliminate residual SFO and to mitigate time-drifting offset. The SFO tracking resolution is 1/4 of the pulse width.

For data retrieval at the overwintering site in Mexico, each mSAIL node is programmed with a predefined rendezvous time, carrier frequency channel (ignoring CFO), and ID to start wireless data offloading to gateways. Butterflies typically form multiple clusters at the overwintering site, and multiple gateways will cover each

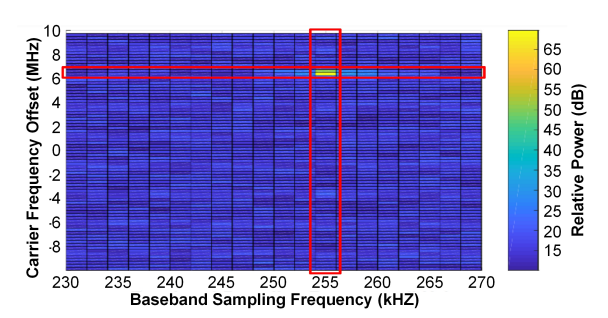


Figure 8: 2-D FFT for CFO and SFO joint estimation.

cluster to reduce the probability of missing packets. mSAIL employs a simple Aloha scheme for accessing the channel without significant medium access control (MAC) overhead so that each node can initiate the message transmission without sensing the channel before transmission. It is the gateway's responsibility to always listen and find the packets (with CFO and SFO) from mSAIL nodes. Packet collision probability is reduced by programming nodes with different carrier frequencies and rendezvous times. Moreover, each mSAIL has a random CFO, thus it is unlikely that multiple nodes use the exact same carrier frequency and start time resulting in packet collision. Each node can be programmed to transmit each unique packet multiple times across different rendezvous times, so that the gateway can recover any missing packets. Even if the gateway misses some packets, our proposed data (de)compression algorithm can recover partial data from successfully received packets. RF interference from other non-mSAIL devices at the overwintering sites is not a major concern since butterfly clusters are in a remote, mountainous area. The proposed Aloha-based MAC is a practical energy-efficient solution for mSAIL when the expected number of nodes at the overwintering site is less than 100.

7 EVALUATION

Various performance evaluations have been run on mSAIL systems as described in this section, including: a) >1-week battery energy autonomy demonstration, b) wireless communication distance evaluation at the overwintering site showing over 150 m NLOS distance, c) 2-day outdoor live monarch demonstration including wireless data transmission, post-processing and localization.

7.1 System Operation Reliability

A series of long term tests was performed on mSAIL to confirm robustness of operation, including: a) 1-week window test to verify energy autonomy and b) 1-week temperature chamber test to verify reliable operation over wide temperature ranges and further confirm energy autonomy under artificial light control.

An mSAIL system mounted on a PGA package for handling was placed in a window for one week along with a cm-scale commercial sensor for independent monitoring of light and temperature. The battery voltage was radioed out periodically. Lowest battery voltages of 4.05 V were observed at night while values of 4.25 V, indicating full recharge, were observed during the day. Fig. 9 shows 1-week of battery and light levels readings. Temperatures in the window varied between 14 $^{\circ}\mathrm{C}$ and 56 $^{\circ}\mathrm{C}$, demonstrating energy-autonomous operation under normal outdoor light conditions.

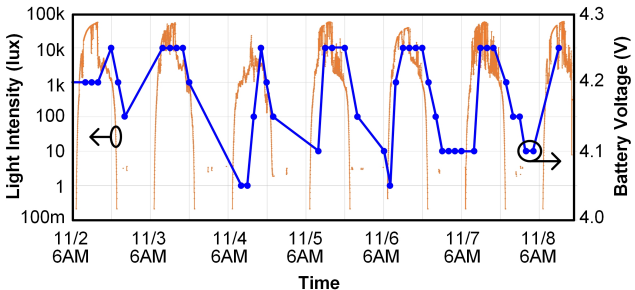


Figure 9: 7-day battery voltage vs. light level.

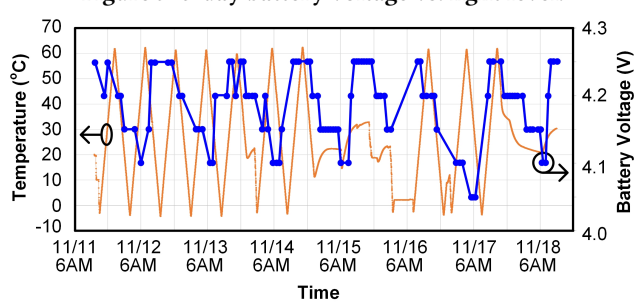


Figure 10: 7-day battery voltage vs. temperature.

Testing operation over temperature is an important part of the mSAIL reliability evaluation due to the large variation in battery internal resistance. Further, the temperature dependence of power management introduces complexity and risk of failure. To test this, an mSAIL system was placed in a temperature chamber for one week along with a cm-scale commercial sensor for light and temperature monitoring in controlled conditions. The temperature was repeatedly swept between -5 and 60 $^{\circ}$ C. A \sim 5 klux light source was turned on for 12 hours per day in the chamber in order to charge the mSAIL battery. Fig. 10 shows the battery level and temperature over the course of the 1-week test. This test also shows the expected energy-autonomous operation over a wide temperature range and lower than expected light levels as typical outdoor light well exceeds 5 klux.

In addition to these full system tests, various subsystems were tested, including a software test which demonstrated over one month of bug-free operation on a debug, wired system.

7.2 Wireless Communication Evaluation

The mSAIL radio transmission distance was tested at two locations. First, in an unobstructed outdoor environment, mSAIL was placed on a pole such that it was an average 20 m higher than the gateway in order to emulate conditions at the overwintering site when a monarch will be in a tall conifer. Results of the test are shown in Fig. 11 (a). A 75 cm Yagi antenna with 11 dBi gain was attached to the gateway. Transmission was line-of-sight up to 494 m. A similar test was performed in a heavily wooded area at the overwintering site in Mexico, shown in Fig. 11 (b) using a 135 cm Yagi with 15 dBi gain which showed excellent results at 150 m with a low (<5%) packet loss. In both cases, the mSAIL was powered by attaching larger batteries using 10 mm leads to allow for longer operation duration under continuous radio transmission for ease of testing. However, in separate testing this was shown not to impact radio distance noticeably.

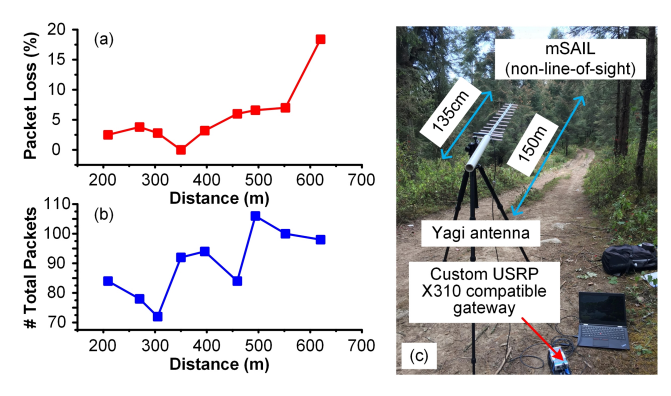


Figure 11: RF communication distance test. (a) Result from the open-area test; (b) Test in wooded area.

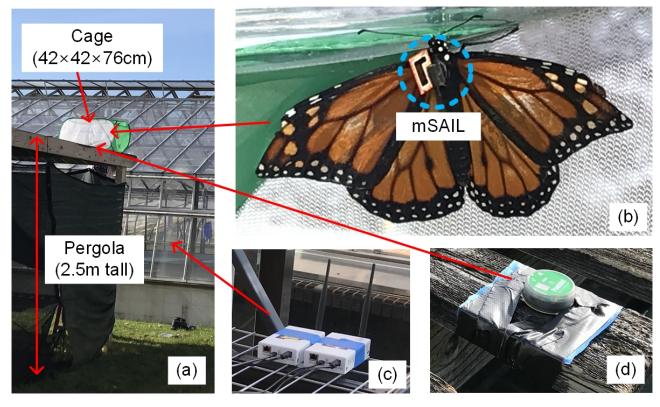


Figure 12: Testing setup for the outdoor botanical garden test. (a) Overview; (b) mSAIL on monarch; (c) Gateway; (d) Centimeter-scale commercial sensor.

Our approach leverages the fact that monarchs cluster at impressive densities at the Mexican overwintering sites. The median density estimate is 20 million butterflies (range 6-60 million) per hectare $(10,000 \text{ m}^2)$ [50]. Therefore, even with hundreds of meters of communication range, we expect to cover millions of butterflies.

7.3 Live Monarch Localization

Full system operation of mSAIL was demonstrated attached to a live monarch butterfly in a botanical garden, as shown in Fig. 12. The butterfly is kept in an outdoor, $42 \times 42 \times 76$ cm cage, positioned on a 2.5 m tall pergola such that the cage is not shaded by nearby buildings, on November 6th and 7th, 2020, which is during the monarch migration season. The monarch was able to feed *ad libitum* on butterfly nectar. For reference measurements, cm-scale sensors [40] were placed in the cage and outside on the pergola. A receiving gateway with a 7" omnidirectional whip antenna was mounted 8 m away in a nearby enclosed structure to receive the transmitted data regardless of weather conditions.

7.3.1 Impact on monarch butterfly. Monarchs were tested and found to reliably carry prototype mSAILs for four weeks when attached to the thorax using a cyanoacrylate-based adhesive (Loctite 401), matching the average lifespan of captive-reared butterflies. Monarchs carrying loggers could open and close their wings normally (both behaviors are important for proper thermoregulation),

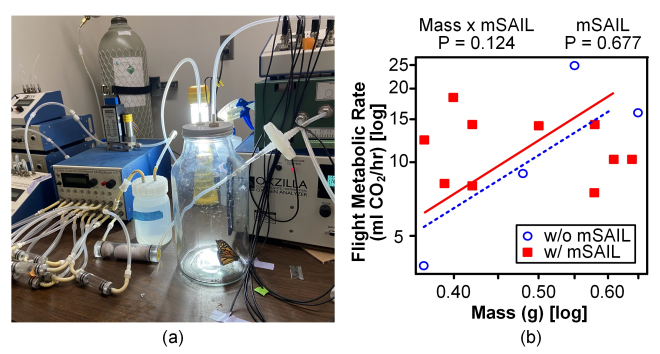


Figure 13: CO₂ respirometry. (a) Setup; (b) Result.

show no noticeable flight impairment, and mate and copulate successfully. Also, we performed flow-through $\rm CO_2$ respirometry on monarchs carrying a prototype mSAIL (compared to controls without the logger) to estimate the effect of the system load on flight metabolism. As shown in Fig. 13, system attachment showed neither a significantly different mass relationship from control (P=0.124), nor a significant change of flight metabolic rate (P=0.677). Because the data in this preliminary study was limited, further studies on the impact of long-distance flight and aerodynamics, as well as the robustness of the mSAIL over a 3-month period, are warranted and planned.

7.3.2 Impact on environment. Our tests did not cover the impact of mSAIL on the environment. Further studies need to be conducted on areas such as the impact on predators and the accumulation of technical waste at overwintering sites. However, since an estimated 10% of monarchs reach the overwintering site, most of which successfully leave with the mSAILs still attached, only a small fraction of mSAILs will be deposited over a relative large area (compared to the mSAIL's size), reducing the expected impact.

7.3.3 Light & temperature measurement results. Fig. 14 shows temperature data transmitted from mSAIL mounted on the monarch. Data is also shown for the cm-scale sensor mounted on the pergola, along with the difference between the two sensors' measures. Temperature data agrees very well between 6 PM and 6 AM with differences of no more than 2 °C. During primary daylight hours both sensors can be exposed directly to sunlight which can cause large local heating compared to ambient shade temperatures. While the cm-scale sensor was mounted on the pergola, facing up, the mSAIL was attached to the monarch which, though caged, could change orientation with respect to the sun and also close its wings at times, thereby covering the sensor. Therefore, differences in daytime temperatures are expected. For these reasons, and because butterflies will travel during the day, only nighttime temperature readings (16 hours) are used in the DNN localization algorithm.

Fig. 15 shows the 2-day light data from the same mSAIL system and the same cm-scale sensor. Note that mSAIL is programmed to gather light data only during daytime and sunrise/sunset intervals. Also, the cm-scale sensor's minimum light reading is zero which cannot be plotted on the log scale. The data shows good agreement during sunrise and sunset times. Some of the differences during day time are the results of difference in orientation between the fixed cm sensor and the mSAIL. The cm sensor always pointed upward while mSAIL orientation depended on the position of the monarch.

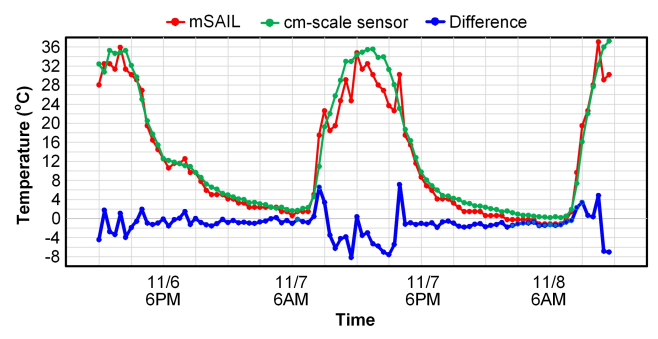


Figure 14: 2-day temperature: mSAIL vs. ref. sensor.

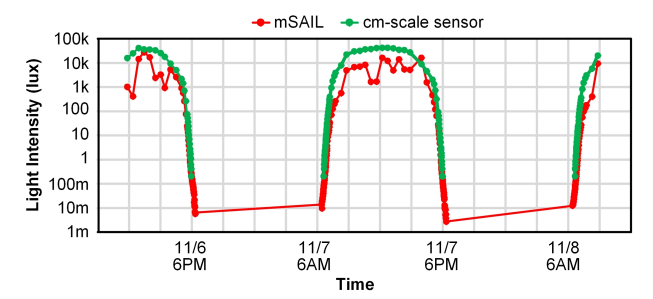


Figure 15: 2-day light data: mSAIL vs. ref. sensor.

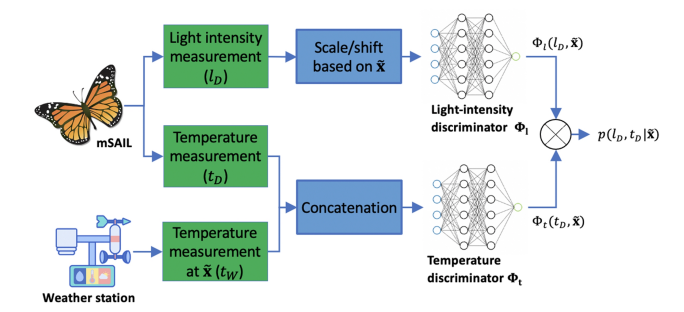


Figure 16: DNN localization algorithm using mSAIL light and temperature measurement data.

However, the neural network localization algorithm mostly relies on measurements surrounding sunrise and sunset. In addition, in practice, measurements during the day are less relevant since the monarch could be traveling and, hence, not at a fixed location. In addition, to confirm accuracy of the light readings, mSAIL was calibrated and tested with controlled light prior to the live monarch experiment. The resulting fit had an R² value of 0.9982.

7.3.4 Localization from mSAIL collected data. The quality of our measurements was evaluated using the localization algorithm introduced in [59]. Although it is possible to apply different localization algorithms using mSAIL-collected data, we chose the same algorithm proposed in [59] to evaluate its data quality compared to the output obtained from the reference commercial sensor.

For any given location x (latitude, longitude), the goal is to estimate the likelihood of observed light intensity l_D and temperature t_D at day D (i.e., $\hat{p}(l_D, t_D|x)$). Then, given a set of location candidates X, the location estimation \hat{x}_D at day D is the one producing the maximum likelihood, as shown in (1).

$$\hat{x}_D = \operatorname*{arg\,max} \hat{p}(l_D, t_D | x) \tag{1}$$
 The likelihood estimation is achieved using two binary discrimi-

nator neural networks: light intensity discriminator Φ_I and temperature discriminator Φ_t as shown in Fig. 16. Φ_t and Φ_t are trained using the volunteer data collected by off-the-shelf cm-scale sensors [40] (as mSAIL emulators) from 2018 to 2020 at 135 locations with ground-truth GPS coordinates for 3053 days to produce a high score when the input (temperature or light) matches the data property expected at the coordinate x. For Φ_I , the input is the mSAIL (or cm-scale sensor) light data l_D for the day D and the neural network produces high output when the data matches the expected light curve at a particular coordinate x. Φ_t takes the pair of the actual mSAIL (or cm-scale sensor) temperature data t_D and the weather station temperature data reported for a particular coordinate x on the same day D. Its output is high when both t_D and weather station data are from the same coordinate and day. Φ_I and Φ_t outputs are evaluated for the measured mSAIL or cm-scale sensor data by sweeping possible coordinates x in the search grid. Since Sigmoid is used as the final activation function, the outputs $\Phi_I(l_D, x)$ and $\Phi_t(t_D, x)$ can be interpreted as likelihoods. Then, with a simplifying assumption that the light and temperature observations are independent, the likelihood is estimated by simply multiplying the neural network outputs [59], which is:

$$\hat{p}(l_D, t_D|x) \approx \hat{p}(l_D|x)\hat{p}(t_D|x) \approx \Phi_l(l_D, x)\Phi_t(t_D, x)$$
 (2)

For the live monarch mSAIL evaluation conducted on Nov. 6th and 7th in 2020, the light and temperature data were wirelessly retrieved from the mSAIL unit and the butterfly was localized using the above method. Note that mSAIL collected data was first decompressed and resampled to reverse the adaptive sampling and data compression described in Section 5. We then applied a linear interpolation to resample decompressed mSAIL measurements so that they have the same sampling rate as the reference cm-scale sensors used in DNN training. We evaluate our 2-day measurements in a grid surrounding the ground-truth location with a range of [-15, 15] degree in latitude and longitude and a resolution of 0.25 degree. The likelihood (i.e., DNN outputs) for the grid points are visualized as heatmaps shown in Fig. 17 where the center of the graph is the ground-truth location. It is observed that light intensity alone is able to provide accurate longitude estimation and that temperature significantly refines the latitude estimation. The maximum likelihood estimations marked in Fig. 17 provide an absolute error of $0.07^{\circ}/0.26^{\circ}$ in longitude and $0.03^{\circ}/0.40^{\circ}$ in latitude for the first/second day, which translates to a maximum error of 21.4 km and 44.5 km in longitude and latitude and aligns with the accuracy reported in [59] evaluated with the cm-scale sensors.

To validate that the proposed data compression and adaptive resampling technique does not degrade the localization accuracy, we applied the same compression and sampling technique to the volunteer cm-scale sensor data and compared the localization accuracy with the original uncompressed data. Fig. 18 confirms that the proposed compression and dynamic sampling algorithm successfully captures the most relevant features, thus it exhibits negligible localization accuracy difference.

It is worth noting that the butterfly was stationary for the 2-day outdoor test and there can be differences between data collected

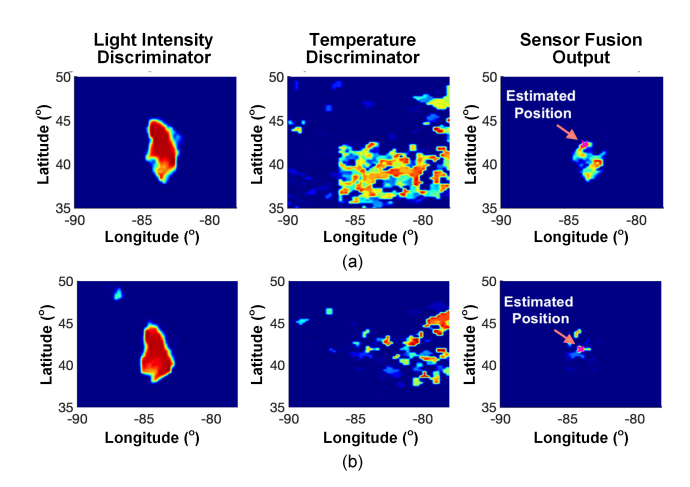


Figure 17: Localization likelihood output for two different days (a) and (b). Center of each heatmap is the ground-truth. Maximum error after sensor fusion is 21.4 km and 44.5 km in longitude and latitude.

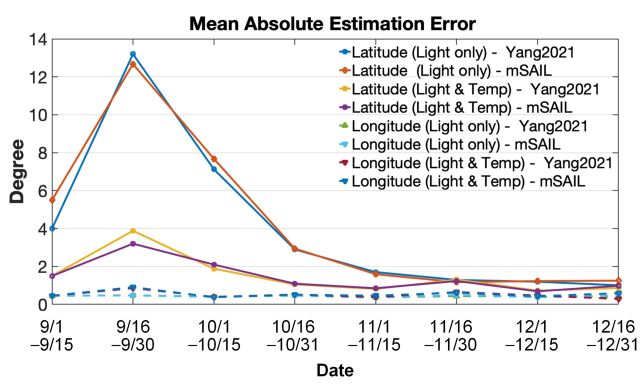


Figure 18: MSE of latitude and longitude evaluated biweekly with mSAIL data compression vs. original uncompressed cm-scale sensor data in [59].

from stationary vs. migrating butterflies. Analyzing the differences needs further investigation and it is left as future work.

8 RELATED WORK

The lightest commercial GPS-based device for animal tracking is PinPoint-10 (1.1 g) by Lotek Wireless for tracking Ovenbirds (20 g) [15]. This device is suitable for animals heavier than 20 g, including 1300 bird [3] and 300 mammal species [2]. The ICARUS global monitoring system (Max Planck Gesellschaft) developed a 5 g unit (12 cm antenna) with promises to reach 1 g [55]. It measures environmental variables including light level, temperature, and pressure, as well as acceleration for behavioral and physiological inference. However, these tracking systems are $16\times$ heavier than mSAIL and $2\times$ heavier than a monarch butterfly itself.

Today's lightest geolocation-based insect tracking devices rely only on light to estimate sunrise/sunset times and weigh >300 mg (Intigeo by Migrate Technology [21]). They are still too heavy for a monarch. Also, the system lifetime is finite by relying on a battery without energy-harvesting, and requires the device to be physically retrieved to read out data.

Miniature embedded devices have been proposed with cm or even mm scales to be mounted on insects. A cm-scale wireless steerable vision system (84 mg, wireless camera part only) records images on a beetle with wireless communication distance of 120 m at 4.4–18 mW [19]. An innovative device of 4.6×6.8 mm and 38 mg uses wireless power transfer and communication for a dragonfly, with the operating range of 1.5 m at 1.2 mW [51]. These devices demonstrate electronic systems mountable on small insects, but do not incorporate localization techniques. On a bee, a 102 mg, 6.1×6.4 mm system performs RF-based localization with 80 m distance and measures humidity, temperature, and light intensity [20]. Its system lifetime is seven hours and consumes 138 μ A (1.6 mA in active and 100 μ A in sleep mode). This technology is a promising solution for its target application (smart farming), where the insect is always near an access-point setup. However, its localization approach cannot support the long distance migration of the monarch. Also, its lifetime could be extended by RF or solar harvesting although full energy autonomy might be difficult. The wireless communication distance is also limited to 5 m. Recently, as a part of work in [18], a 98 mg system significantly increases the system lifetime to 1.3-2.5 years by reducing its sleep power to 35 nA using a timer. It also improves the wireless communication distance to 1 km. However, its localization technique is not applicable to monarchs migrating 4,000 km.

As far as devices lighter than mSAIL, passive RFID-based tags (~5 mg) have been used to monitor local movement patterns of individual insects (e.g. [12]), but these passive tags do not actively measure and store data, and they operate over a highly restrictive communication range.

9 CONCLUSION

This paper proposes mSAIL, $8\times8\times2.6$ mm and 62 mg embedded system for monarch butterfly migration tracking with previously developed, custom-fabricated solar energy harvester, ultra-low power processor, light/temperature sensors, and wireless transceiver ICs, all integrated within a 3D stacked form-factor. The proposed system is designed to record and compress light and temperature data during the entire 3-month migration path while harvesting solar energy, and wirelessly transmitting the data at the overwintering site in Mexico to reconstruct the complete migration trajectory using a deep learning-based sensor fusion localization algorithm. An initial 2-day trial experiment of mSAIL attached on a live butterfly demonstrates the feasibility of individual monarch butterfly localization and tracking using an electronic device for the first time.

ACKNOWLEDGMENTS

We are grateful to the Monarch Butterfly Biosphere Reserve Director (Felipe Martínez Meza), staff, and community partners for granting access to the overwintering colony. We thank Dr. M. Isabel Ramírez and students for assistance at the overwintering site. This work was funded in part by Monarch Butterfly Fund Flight Challenge, National Geographic, Mcubed, NSF DBI IIBR (#2045017 & #2043017), and NSF UNVEIL IOS (#1736249). The authors thank all volunteers for data collection from 2018–2020.

REFERENCES

- ARM. [n.d.]. ARM 180nm Ultra Low Power Platform. https://developer.arm.com/ documentation/pfl0307/latest. [Online; accessed 20-March-2021].
- [2] Tim Blackburn and Kevin Gaston. 1998. The distribution of mammal body masses. Diversity and Distributions 4, 3 (1998), 121–133. https://doi.org/10.1046/j.1365-2699.1998.00015.x arXiv:https://onlinelibrary.wiley.com/doi/pdf/10.1046/j.1365-2699.1998.00015.x
- [3] Tim M. Blackburn and Kevin J. Gaston. 1994. The Distribution of Body Sizes of the World's Bird Species. Oikos 70, 1 (1994), 127–130. http://www.jstor.org/ stable/3545707
- [4] J. H. Boyle, H. J. Dalgleish, and J. R. Puzey. 2019. Monarch butterfly and milkweed declines substantially predate the use of genetically modified crops. *Proceedings* of the National Academy of Sciences 116, 8 (2019), 3006–3011. https://doi.org/10. 1073/pnas.1811437116 arXiv:https://www.pnas.org/content/116/8/3006.full.pdf
- [5] R. B. Brander and W. W. Cochran. 1969. Wildlife Management Techniques. The Wildlife Society, Washington, DC, USA, Name of chapter: Radio location telemetry (Inbook-w-chap-w-type), 95–103.
- [6] Larry J. Brindza, L. Brower, A. Davis, and T. V. Hook. 2008. COMPARATIVE SUC-CESS OF MONARCH BUTTERFLY MIGRATION TO OVERWINTERING SITES IN MEXICO FROM INLAND AND COASTAL SITES. Journal of the Lepidopterists' Society 62, 4, 189–200.
- [7] William H. Calvert, Lee E. Hedrick, and Lincoln P. Brower. 1979. Mortality of the Monarch Butterfly (Danaus plexippus L.): Avian Predation at Five Overwintering Sites in Mexico. Science 204, 4395 (1979), 847–851. https://doi.org/10.1126/science. 204.4395.847 arXiv:https://science.sciencemag.org/content/204/4395/847.full.pdf
- [8] Jason W. Chapman, Rebecca L. Nesbit, Laura E. Burgin, Don R. Reynolds, Alan D. Smith, Douglas R. Middleton, and Jane K. Hill. 2010. Flight Orientation Behaviors Promote Optimal Migration Trajectories in High-Flying Insects. Science 327, 5966 (2010), 682–685. https://doi.org/10.1126/science.1182990 arXiv:https://science.sciencemag.org/content/327/5966/682.full.pdf
- [9] Y. Chen, N. Chiotellis, L. Chuo, C. Pfeiffer, Y. Shi, R. G. Dreslinski, A. Grbic, T. Mudge, D. D. Wentzloff, D. Blaauw, and H. S. Kim. 2016. Energy-Autonomous Wireless Communication for Millimeter-Scale Internet-of-Things Sensor Nodes. IEEE Journal on Selected Areas in Communications 34, 12 (2016), 3962–3977. https://doi.org/10.1109/JSAC.2016.2612041
- [10] L. Chuo, Y. Shi, Z. Luo, N. Chiotellis, Z. Foo, G. Kim, Y. Kim, A. Grbic, D. Wentzloff, H. Kim, and D. Blaauw. 2017. 7-4 A 915MHz asymmetric radio using Q-enhanced amplifier for a fully integrated 3×3×3mm3 wireless sensor node with 20m non-line-of-sight communication. In 2017 IEEE International Solid-State Circuits Conference (ISSCC). 132–133. https://doi.org/10.1109/ISSCC.2017.7870296
- [11] CYMBET Corporation. [n.d.]. ENERCHIP™ SMART SOLID STATE BATTERIESs. https://www.cymbet.com/products/enerchip-solid-state-batteries/. [Online; accessed 20-March-2021].
- [12] Paulo De Souza, Peter Marendy, Karien Barbosa, Setia Budi, Pascal Hirsch, Nasiha Nikolic, Tom Gunthorpe, Gustavo Pessin, and Andrew Davie. 2018. Low-Cost Electronic Tagging System for Bee Monitoring. Sensors 18, 7 (2018). https://doi.org/10.3390/s18072124
- [13] R. G. Dreslinski, M. Wieckowski, D. Blaauw, D. Sylvester, and T. Mudge. 2010. Near-Threshold Computing: Reclaiming Moore's Law Through Energy Efficient Integrated Circuits. *Proc. IEEE* 98, 2 (2010), 253–266. https://doi.org/10.1109/ IPROC.2009.2034764
- [14] Ettus Research. [n.d.]. USRP X310. https://www.ettus.com/all-products/x310-kit/. [Online; accessed 20-March-2021].
- [15] Michael Hallworth and Peter Marra. 2015. Miniaturized GPS Tags Identify Non-breeding Territories of a Small Breeding Migratory Songbird. Scientific Reports 5 (06 2015), 11069. https://doi.org/10.1038/srep11069
- [16] Gao Hu, Ka S. Lim, Nir Horvitz, Suzanne J. Clark, Don R. Reynolds, Nir Sapir, and Jason W. Chapman. 2016. Mass seasonal bioflows of high-flying insect migrants. *Science* 354, 6319 (2016), 1584–1587. https://doi.org/10.1126/science.aah4379 arXiv:https://science.sciencemag.org/content/354/6319/1584.full.pdf
- [17] David A. Huffman. 1952. A Method for the Construction of Minimum-Redundancy Codes. Proceedings of the Institute of Radio Engineers 40, 9 (September 1952) 1098–1101.
- [18] Vikram Iyer, Maruchi Kim, Shirley Xue, Anran Wang, and Shyamnath Gollakota. 2020. Airdropping Sensor Networks from Drones and Insects. In Proceedings of the 26th Annual International Conference on Mobile Computing and Networking (London, United Kingdom) (MobiCom '20). Association for Computing Machinery, New York, NY, USA, Article 61, 14 pages. https://doi.org/10.1145/3372224.3419981
- [19] Vikram Iyer, Ali Najafi, Johannes James, Sawyer Fuller, and Shyamnath Gollakota. 2020. Wireless steerable vision for live insects and insect-scale robots. Science Robotics 5, 44 (2020). https://doi.org/10.1126/scirobotics.abb0839 arXiv:https://robotics.sciencemag.org/content/5/44/eabb0839.full.pdf
- [20] Vikram İyer, Rajalakshmi Nandakumar, Anran Wang, Sawyer B. Fuller, and Shyamnath Gollakota. 2019. Living IoT: A Flying Wireless Platform on Live Insects. In The 25th Annual International Conference on Mobile Computing and Networking (Los Cabos, Mexico) (MobiCom '19). Association for Computing Machinery, New York, NY, USA, Article 5, 15 pages. https://doi.org/10.1145/

- 3300061 3300136
- [21] James W. Fox. 2018. Intigeo series geolocator. http://www.migratetech.co.uk/ IntigeoSummary.pdf. [Online; accessed 20-March-2021].
- [22] S. Jeong, Z. Foo, Y. Lee, J. Sim, D. Blaauw, and D. Sylvester. 2014. A Fully-Integrated 71 nW CMOS Temperature Sensor for Low Power Wireless Sensor Nodes. *IEEE Journal of Solid-State Circuits* 49, 8 (2014), 1682–1693. https://doi.org/10.1109/JSSC.2014.2325574
- [23] W. Jung, J. Gu, P. D. Myers, M. Shim, S. Jeong, K. Yang, M. Choi, Z. Foo, S. Bang, S. Oh, D. Sylvester, and D. Blaauw. 2016. 8.5 A 60%-efficiency 20nW-500μW trioutput fully integrated power management unit with environmental adaptation and load-proportional biasing for IoT systems. In 2016 IEEE International Solid-State Circuits Conference (ISSCC). 154–155. https://doi.org/10.1109/ISSCC.2016. 7417953
- [24] W. Jung, S. Oh, S. Bang, Y. Lee, Z. Foo, G. Kim, Y. Zhang, D. Sylvester, and D. Blaauw. 2014. An Ultra-Low Power Fully Integrated Energy Harvester Based on Self-Oscillating Switched-Capacitor Voltage Doubler. *IEEE Journal of Solid-State Circuits* 49, 12 (2014), 2800–2811. https://doi.org/10.1109/JSSC.2014.2346788
- [25] Samantha M. Knight, Grace M. Pitman, D. T. Tyler Flockhart, and D. Ryan Norris. 2019. Radio-tracking reveals how wind and temperature influence the pace of daytime insect migration. *Biology Letters* 15, 7 (2019), 20190327. https://doi.org/10.1098/rsbl.2019.0327 arXiv:https://royalsocietypublishing.org/doi/pdf/10.1098/rsbl.2019.0327
- [26] Y. Kuo, P. Pannuto, G. Kim, Z. Foo, İ. Lee, B. Kempke, P. Dutta, D. Blaauw, and Y. Lee. 2014. MBus: A 17.5 pJ/bit/chip portable interconnect bus for millimeter-scale sensor systems with 8 nW standby power. In Proceedings of the IEEE 2014 Custom Integrated Circuits Conference. 1–4. https://doi.org/10.1109/CICC.2014.6946046
- [27] Chi Lam, Anders Nielsen, and John Sibert. 2008. Improving light and temperature based geolocation by unscented Kalman filtering. Fisheries Research 91 (05 2008), 15–25. https://doi.org/10.1016/j.fishres.2007.11.002
- [28] Chi Lam, Anders Nielsen, and John Sibert. 2010. Incorporating sea-surface temperature to the light-based geolocation model TrackIt. Marine Ecology Progress Series 419 (11 2010), 71–84. https://doi.org/10.3354/meps08862
- 29] I. Lee, G. Kim, E. Moon, S. Jeong, D. Kim, J. Phillips, and D. Blaauw. 2018. A 179-Lux Energy-Autonomous Fully-Encapsulated 17-mm3 Sensor Node with Initial Charge Delay Circuit for Battery Protection. In 2018 IEEE Symposium on VLSI Circuits. 251–252. https://doi.org/10.1109/VLSIC.2018.8502287
- [30] I. Lee, E. Moon, Y. Kim, J. Phillips, and D. Blaauw. 2019. A 10mm3 Light-Dose Sensing IoT2 System With 35-To-339nW 10-To-300klx Light-Dose-To-Digital Converter. In 2019 Symposium on VLSI Circuits. C180–C181. https://doi.org/10. 23919/VLSIC.2019.8778007
- [31] Kenneth J. Lohmann and Catherine M. F. Lohmann. 2019. There and back again: natal homing by magnetic navigation in sea turtles and salmon. Journal of Experimental Biology 222, Suppl 1 (2019). https://doi.org/10.1242/jeb.184077 arXiv:https://jeb.biologists.org/content/222/Suppl_1/jeb184077.full.pdf
- [32] Lotek. 2020. PinPoint GPS Beacon for birds & bats. https://www.lotek.com/products/pinpoint-gps-beacon/. [Online; accessed 20-March-2021].
- [33] Filip Maksimovic, Brad Wheeler, David C. Burnett, Osama Khan, Sahar Mesri, Ioana Suciu, Lydia Lee, Alex Moreno, Arvind Sundararajan, Bob Zhou, Rachel Zoll, Andrew Ng, Tengfei Chang, Xavier Villajosana, Thomas Watteyne, Ali Niknejad, and Kristofer S. J. Pister. 2019. A Crystal-Free Single-Chip Micro Mote with Integrated 802.15.4 Compatible Transceiver, sub-mW BLE Compatible Beacon Transmitter, and Cortex M0. In 2019 Symposium on VLSI Circuits. C88-C89. https://doi.org/10.23919/VLSIC.2019.8777971
- [34] MEDIATEK Labs. [n.d.]. MT3339. https://labs.mediatek.com/en/chipset/MT3339. [Online; accessed 20-March-2021].
- [35] Monarch Watch. [n.d.]. Tagging Monarchs. https://monarchwatch.org/tagging/. [Online; accessed 20-March-2021].
- [36] Eunseong Moon, Inhee Lee, David Blaauw, and Jamie D. Phillips. 2019. High-efficiency photovoltaic modules on a chip for millimeterscale energy harvesting. Progress in Photovoltaics: Research and Applications 27, 6 (2019), 540–546. https://doi.org/10.1002/pip.3132 arXiv:https://onlinelibrary.wiley.com/doi/pdf/10.1002/pip.3132
- [37] NFSF. [n.d.]. Monarch Butterfly Conservation Fund. https://www.nfwf.org/ sites/default/files/monarch/Documents/three-year-report.pdf. [Online; accessed 20-March-2021].
- [38] Anders Nielsen, Keith A. Bigelow, Michael K. Musyl, and John R. Sibert. 2006. Improving light-based geolocation by including sea surface temperature. Fisheries Oceanography 15, 4 (2006), 314–325. https://doi.org/10.1111/j.1365-2419.2005.00401.x arXiv:https://onlinelibrary.wiley.com/doi/pdf/10.1111/j.1365-2419.2005.00401.x
- [39] S. Oh, M. Cho, X. Wu, Y. Kim, L. Chuo, W. Lim, P. Pannuto, S. Bang, K. Yang, H. Kim, D. Sylvester, and D. Blaauw. 2019. IoT2 — the Internet of Tiny Things: Realizing mm-Scale Sensors through 3D Die Stacking. In 2019 Design, Automation Test in Europe Conference Exhibition (DATE). 686–691. https://doi.org/10.23919/ DATE.2019.8715201
- [40] ONSET. [n.d.]. HOBO Pedant MX Temperature/Light Data Logger. https://www.onsetcomp.com/products/data-loggers/mx2202/. [Online; accessed 20-March-2021].

- [41] P. Pannuto, Y. Lee, Y. Kuo, Z. Foo, B. Kempke, G. Kim, R. G. Dreslinski, D. Blaauw, and P. Dutta. 2015. MBus: An ultra-low power interconnect bus for next generation nanopower systems. In 2015 ACM/IEEE 42nd Annual International Symposium on Computer Architecture (ISCA). 629–641. https://doi.org/10.1145/2749469. 2750376
- [42] P. Pannuto, Y. Lee, Y. Kuo, Z. Foo, B. Kempke, G. Kim, R. G. Dreslinski, D. Blaauw, and P. Dutta. 2016. MBus: A System Integration Bus for the Modular Microscale Computing Class. *IEEE Micro* 36, 3 (2016), 60–70. https://doi.org/10.1109/MM. 2016.41
- [43] Gretta T. Pecl, Miguel B. Araújo, Johann D. Bell, Julia Blanchard, Timothy C. Bonebrake, I-Ching Chen, Timothy D. Clark, Robert K. Colwell, Finn Danielsen, Birgitta Evengård, Lorena Falconi, Simon Ferrier, Stewart Frusher, Raquel A. Garcia, Roger B. Griffis, Alistair J. Hobday, Charlene Janion-Scheepers, Marta A. Jarzyna, Sarah Jennings, Jonathan Lenoir, Hlif I. Linnetved, Victoria Y. Martin, Phillipa C. McCormack, Jan McDonald, Nicola J. Mitchell, Tero Mustonen, John M. Pandolfi, Nathalie Pettorelli, Ekaterina Popova, Sharon A. Robinson, Brett R. Scheffers, Justine D. Shaw, Cascade J. B. Sorte, Jan M. Strugnell, Jennifer M. Sunday, Mao-Ning Tuanmu, Adriana Vergés, Cecilia Villanueva, Thomas Wernberg, Erik Wapstra, and Stephen E. Williams. 2017. Biodiversity redistribution under climate change: Impacts on ecosystems and human well-being. Science 355, 6332 (2017). https://doi.org/10.1126/science.aai9214 arXiv:https://science.sciencemag.org/content/355/6332/eaai9214.full.pdf
- [44] Grant L. Pilkay, Francis P. F. Reay-Jones, and Jeremy K. Greene. 2013. Harmonic Radar Tagging for Tracking Movement of Nezara viridula (Hemiptera: Pentatomidae). Environmental Entomology 42, 5 (10 2013), 1020–1026. https://doi.org/10.1603/EN13095 arXiv:https://academic.oup.com/ee/article-pdf/42/5/1020/18313078/ee42-1020.pdf
- [45] D. Psychoudakis, W. Moulder, C. Chen, H. Zhu, and J. L. Volakis. 2008. A Portable Low-Power Harmonic Radar System and Conformal Tag for Insect Tracking. IEEE Antennas and Wireless Propagation Letters 7 (2008), 444–447. https://doi. org/10.1109/LAWP.2008.2004512
- [46] Eldar Rakhimberdiev, David Winkler, Eli Bridge, Nathaniel Seavy, Daniel Sheldon, Theunis Piersma, and Anatoly Saveliev. 2015. A hidden Markov model for reconstructing animal paths from solar geolocation loggers using templates for light intensity. Movement Ecology 3 (10 2015). https://doi.org/10.1186/s40462-015-0062-5
- [47] L. G. Salem and P. P. Mercier. 2014. A Recursive Switched-Capacitor DC-DC Converter Achieving 2^N – 1 Ratios With High Efficiency Over a Wide Output Voltage Range. *IEEE Journal of Solid-State Circuits* 49, 12 (2014), 2773–2787. https://doi.org/10.1109/JSSC.2014.2353791
- [48] U.S. Forest Service. [n.d.]. Migration and Overwintering. https://www.fs.fed.us/wildflowers/pollinators/Monarch_Butterfly/migration/index.shtml#:~: text=Monarchs%20can%20travel%20between%2050,265%20miles%20in%20one%20day. [Online; accessed 20-March-2021].
- [49] P. Taylor, T. Crewe, S. Mackenzie, D. Lepage, Y. Aubry, Z. Crysler, G. Finney, C. Francis, C. Guglielmo, D. Hamilton, R. L. Holberton, P. H. Loring, G. W. Mitchell, D. Norris, J. Paquet, R. A. Ronconi, J. Smetzer, P. A. Smith, L. J. Welch, and B. K. Woodworth. 2017. The Motus Wildlife Tracking System: a collaborative research network to enhance the understanding of wildlife movement. Avian Conservation and Ecology 18 (03 2017), 8. https://doi.org/10.5751/ACE-00953-120108
- [50] Wayne Thogmartin, Jay Diffendorfer, Laura López-Hoffman, Karen Oberhauser, John Pleasants, Brice Semmens, Darius Semmens, Orley Taylor, and Ruscena Wiederholt. 2017. Density estimates of monarch butterflies overwintering in central Mexico. Peerf 5 (04 2017). https://doi.org/10.7717/peerj.3221
- [51] S. J. Thomas, R. R. Harrison, A. Leonardo, and M. S. Reynolds. 2012. A Battery-Free Multichannel Digital Neural/EMG Telemetry System for Flying Insects. *IEEE Transactions on Biomedical Circuits and Systems* 6, 5 (2012), 424–436. https://doi.org/10.1109/TBCAS.2012.2222881
- [52] Kasper Thorup, Anders P. Tøttrup, Mikkel Willemoes, Raymond H. G. Klaassen, Roine Strandberg, Marta Lomas Vega, Hari P. Dasari, Miguel B. Araújo, Martin Wikelski, and Carsten Rahbek. 2017. Resource tracking within and across continents in long-distance bird migrants. Science Advances 3, 1 (2017). https://doi.org/10.1126/sciadv.1601360 arXiv:https://advances.sciencemag.org/content/3/1/e1601360.full.pdf
- [53] Omar Vidal and Eduardo Rendón-Salinas. 2014. Dynamics and trends of overwintering colonies of the monarch butterfly in Mexico. *Biological Conservation* 180 (2014), 165–175. https://doi.org/10.1016/j.biocon.2014.09.041
- [54] Caitlin Ware. 2018. ISU student using radio telemetry to track monarch butterflies. Retrieved March 20, 2021 from https://www.amestrib.com/news/20180713/isu-student-using-radio-telemetry-to-track-monarch-butterflies
- [55] Martin Wikelski, Roland W. Kays, N. Jeremy Kasdin, Kasper Thorup, James A. Smith, and George W. Swenson. 2007. Going wild: what a global small-animal tracking system could do for experimental biologists. *Journal of Experimental Biology* 210, 2 (2007), 181–186. https://doi.org/10.1242/jeb.02629 arXiv:https://jeb.biologists.org/content/210/2/181.full.pdf
- [56] Wikipedia contributors. 2021. Lambert's cosine law Wikipedia, The Free Encyclopedia. https://en.wikipedia.org/w/index.php?title=Lambert%27s_cosine_

- law&oldid=1003633457. [Online; accessed 20-March-2021].
- [57] Wikipedia contributors. 2021. Position of the Sun Wikipedia, The Free Encyclopedia. https://en.wikipedia.org/w/index.php?title=Position_of_the_Sun&oldid=1013011697. [Online; accessed 20-March-2021].
- [58] K. Yang, Q. Dong, W. Jung, Y. Zhang, M. Choi, D. Blaauw, and D. Sylvester. 2017. 9.2 A 0.6nJ -0.22/+0.19°C inaccuracy temperature sensor using exponential subthreshold oscillation dependence. In 2017 IEEE International Solid-State Circuits Conference (ISSCC). 160-161. https://doi.org/10.1109/ISSCC.2017.7870310
- [59] M. Yang, R. Hsiao, G. Carichner, K. Ernst, J. Lim, D. A. Green, I. Lee, D. Blaauw, and H. S. Kim. 2021. Migrating Monarch Butterfly Localization Using Multi-Modal Sensor Fusion Neural Networks. In 2020 28th European Signal Processing Conference (EUSIPCO). 1792–1796. https://doi.org/10.23919/Eusipco47968.2020.9287842
- [60] D. Yoon, T. Jang, D. Sylvester, and D. Blaauw. 2016. A 5.58 nW Crystal Oscillator Using Pulsed Driver for Real-Time Clocks. *IEEE Journal of Solid-State Circuits* 51, 2 (2016), 509–522. https://doi.org/10.1109/JSSC.2015.2501982
- [61] B. Zhai, R. G. Dreslinski, D. Blaauw, T. Mudge, and D. Sylvester. 2007. Energy efficient near-threshold chip multi-processing. In Proceedings of the 2007 international symposium on Low power electronics and design (ISLPED '07). 32–37. https://doi.org/10.1145/1283780.1283789